Uptake of 3,4-methylenedioxymethamphetamine and its related compounds by a proton-coupled transport system in Caco-2 cells

Kenji Kuwayama [a,b,*], Hiroyuki Inoue [a], Tatsuyuki Kanamori [a], Kenji Tsujikawa [a], Hajime Miyaguchi [a], Yuko Iwata [a], Seiji Miyauchi [b], Naoki Kamo [b], Tohru Kishi [a]

[a] *National Research Institute of Police Science, 6-3-1, Kashiwanoha, Kashiwa, Chiba 277-0882, Japan*
[b] *Laboratory of Biophysical Chemistry, Graduate School of Pharmaceutical Sciences, Hokkaido University, Sapporo 060-0812, Japan*

Abstract

3,4-Methylenedioxymethamphetamine (MDMA) is an illegal amphetamine-type stimulant (ATS) that is abused orally in the form of tablets for recreational purposes. The aim of this work is to investigate the absorption mechanism of MDMA and other related compounds that often occur together in ATS tablets, and to determine whether such tablet components interact with each other in intestinal absorption. The characteristics of MDMA uptake by the human intestinal epithelial Caco-2 cell line were investigated. The Michaelis constant and the maximal uptake velocity at pH 6.0 were 1.11 mM and 13.79 nmol/min/mg protein, respectively, and the transport was electroneutral. The initial uptake rate was regulated by both intra- and extracellular pH. MDMA permeation from the apical to the basolateral side was inferior to that in the reverse direction, and a decrease in apical pH enhanced MDMA permeation from the basolateral to the apical side. These facts indicate that this transport system may be an antiporter of H^+. However, under physiological conditions, the proton gradient cannot drive the MDMA uptake because it is inwardly directed. Large concentration differences of MDMA itself drive this antiporter. Various compounds with similar amine moieties inhibited the uptake, but substrates of organic cation transporters (OCT1–3) and an H^+-coupled efflux antiporter, MATE, were not recognized.
© 2007 Elsevier B.V. All rights reserved.

Keywords: MDMA; Amphetamine-type stimulant; Transport; Caco-2 cells; Intestinal absorption

1. Introduction

There has been a considerable increase in the number of seizures induced by amphetamine-type stimulant (ATS) tablets in Japan [1]. The abuse of ATS tablets has become a serious social problem not only in Japan but throughout the world. ATS tablets contain one or more active ingredients such as 3,4-methylenedioxymethamphetamine (MDMA), 3,4-methylenedioxyamphetamine (MDA), 3,4-methylenedioxyethylamphetamine (MDEA), methamphetamine (MA), etc. [2–8]. These components are similar to each other in their pharmacological and toxicological effects, and affect the central nervous system. In addition, the tablets often contain other components having a hallu1cinogenic and/or stimulant effect, such as ketamine and caffeine. Various components in such tablets might interact with each other in the body, leading to serious toxic symptoms.

Because MDMA is the major component in such tablets and can easily be taken orally, it is a matter of urgency for public health and forensic toxicology to elucidate the intestinal absorption mechanism of MDMA and the interactions among components in ATS tablets. To the best of our knowledge, there is little information regarding the intestinal absorption of MDMA [9], although the pharmacological effects of MDMA and the transporters of neurotransmitters such as dopamine and serotonin have been investigated actively using cells that were over-expressing the relevant transporters [10–13].

The aim of this work is to investigate the absorption mechanism of MDMA and its related compounds, and to determine whether such components in tablets interact with each other in intestinal absorption; it is in the intestines where the first steps of pharmacokinetics occur after oral intake. In the present study, the characteristics of MDMA uptake and interference by related

* Corresponding author. Tel.: +81 4 7135 8001; fax: +81 4 7133 9173.
  E-mail address: kuwayama@nrips.go.jp (K. Kuwayama).

compounds are examined using human intestinal Caco-2 cells. Caco-2 cells spontaneously differentiate in culture into polarized cell monolayers with microvilli, which mimic the properties of small intestinal epithelial cells [14,15]. The Caco-2 cell line is a useful model for studying absorption in the small intestine, since these cells retain a number of solute transport systems including those for amino acids [16], sugars [17], phosphates [18], bile acids [19] and dipeptides [20].

We find that the uptake rate of MDMA by Caco-2 cells is electroneutral and is regulated by both intracellular and extracellular pH. An increase in the uptake rate is observed due to intracellular acidification or extracellular alkalinization. Therefore, it seems that the uptake is mediated by an electroneutral 'antiporter' of protons. Under physiological conditions (due to microclimate pH, pH=6 [21]), however, this antiporter seems not to be able to concentrate the substrate because the proton concentration is directed from outside to inside. Nevertheless, we observe the uptake. Thus, we may infer that the substrate (MDMA) enters into cells via this transporter due to its large concentration difference, which induces the uphill proton transport from the inside to the outside of cells. This transport system also recognizes other compounds having amine moiety, such as MDA, MDEA, MA and diphenhydramine.

2. Materials and methods

2.1. Materials

MA and ephedrine (EP) hydrochloride were purchased from Dainippon Pharmaceutical (Osaka, Japan). MDMA, MDA, MDEA and dimethylamphetamine (DMA) were synthesized as reported previously [22–24]. Dulbecco's modified Eagle's medium (DMEM), non-essential amino acids (NEAA), fetal bovine serum (FBS) and trypsin were purchased from Invitrogen Corporation (Carlsbad, CA, USA).

2′,7′-*bis*(Carboxyethyl)-4(5)-carboxyfluorescein-diacetoxymethyl ester (BCECF-AM) was purchased from Dojindo Chemical Co. (Kumamoto, Japan). All other reagents and solvents were purchased from Wako Pure Chemical Industries, Ltd. (Osaka, Japan). Acetonitrile was of high-performance liquid chromatography (HPLC) grade.

2.2. Cell culture

Caco-2 cells at the 13th passage were purchased from the American Type Culture Collection (Manassas, VA). The cells were maintained in DMEM containing 10% FBS and 1% NEAA in an atmosphere of 5% CO_2. They were passaged in 75-cm^2 culture flasks and were fed a fresh medium every 3 days [25]. At approximately 80% confluence, the cells were seeded using 0.02% ethylenediaminetetraacetic acid (EDTA) and 0.05% trypsin at a density of 5.3×10^4 cells/cm^2 on a 60-mm plastic culture dish for the uptake experiment or a 12-mm polyester membrane insert in a 12-well plate (Transwell® insert, membrane pore size; 0.4 μm; Corning, Acton, MA) for the permeation experiment. The cells were cultivated for 7–8 and 20–22 days before they were used for uptake and permeation experiments, respectively. Cells between the 20th and 40th passage were used in the present study.

2.3. Uptake experiments on Caco-2 cell monolayers

The present uptake experiments were performed in a medium consisting of 140 mM NaCl, 3 mM KCl, 1 mM CaCl$_2$, 1 mM MgCl$_2$ and 5 mM D-glucose containing 5 mM 2-(*N*-morpholino)ethanesulfonic acid (MES) (pH 6.0) to imitate the acidic microclimate existing *in vivo* on the small intestine surface [21]. This medium will be referred to as the incubation medium hereafter. After

the culture medium was removed and the cell surface was washed with 1.5 ml of the prewarmed incubation medium (37 °C), the cells were preincubated in the medium for 10 min at 37 °C. The medium was then removed, and the cells were incubated with 1.5 ml of the incubation medium containing MDMA in the presence or absence of various compounds for a designated period (0–3 min) at 37 °C. Next, the medium was removed and the cell surface was washed twice with an ice-cold incubation medium (pH 7.4) containing 5 mM 2-[4-(2-hydroxyethyl)-1-piperazinyl]ethanesulfonic acid (HEPES) instead of 5 mM MES. To measure the uptake at time zero, the incubation medium was removed immediately after its addition and the cell surface was washed twice with the ice-cold incubation medium (pH 7.4) described above. The cells used for the uptake experiments were stored at −30 °C until the following procedures were carried out.

To measure MDMA uptake in the presence of 10 μM oligomycin plus 50 mM 2-deoxyglucose, the cells were preincubated with 1.5 ml of the incubation medium (pH 6.0) containing these additives for 10 min at 37 °C. To examine the influence of ion species in the medium, ion species in the incubation medium (pH 6.0) were replaced and the cells were preincubated with 1.5 ml of the incubation medium (pH 6.0) for 10 min at 37 °C. To examine the influence of the membrane potential, the cells were preincubated with 1.5 ml of the incubation medium (pH 6.0) containing 50 μM valinomycin for 10 min at 37 °C. Diethylpyrocarbonate (DEPC), a specific modifier of histidine residues, was used to examine the contributions of carrier proteins to MDMA uptake. The cells were preincubated in the incubation medium (pH 6.0) containing 2 mM DEPC for 10 min at 37 °C. After removing the medium, the cells were incubated for 3 min at 37 °C with 1.5 ml of the incubation medium (pH 6.0) containing 100 μM MDMA.

To examine the influence of the extracellular pH, the cells were preincubated in the incubation medium (pH 7.4) for 10 min at 37 °C. After removing the medium, the cells were incubated for 3 min at 37 °C with 1.5 ml of the incubation medium (pH 7.4) containing 100 μM MDMA. Carbonyl cyanide *m*-chlorophenylhydrazone (CCCP), a protonophore, and butyrate, a weak acid, were used to examine the influences of the proton electrochemical potential and the intracellular pH. After the cells were preincubated in the incubation medium (pH 6.0) for 10 min at 37 °C, MDMA uptake was measured in the incubation medium (pH 6.0) containing 100 μM MDMA with 50 μM CCCP or 30 mM butyrate (short incubation). Or MDMA uptake was measured in the incubation medium (pH 6.0) containing 100 μM MDMA without CCCP or butyrate after the cells were preincubated with 1.5 ml of the incubation medium (pH 6.0) containing 50 μM CCCP or 30 mM butyrate for 30 min (long incubation) at 37 °C.

In order to examine the effect of intracellular pH on MDMA uptake, intracellular pH was manipulated by treating the cells with NH$_4$Cl or butyric acid. The treatment with NH$_4$Cl was carried out by preincubating the cells for 10 min at 37 °C with the incubation medium (pH 7.4) in the absence (referred to as Acute NH$_4$Cl) or presence (Pre NH$_4$Cl) of 30 mM NH$_4$Cl. After removing the medium, the cells were incubated for 3 min at 37 °C with 1.5 ml of the incubation medium (pH 7.4) containing 100 μM MDMA in the absence (Pre NH$_4$Cl) or presence (Acute NH$_4$Cl) of 30 mM NH$_4$Cl. Another method of changing the intracellular pH was the addition of 30 mM butyric acid. Intracellular pH was estimated by a fluorescent pH probe (BCECF), which is described below.

2.4. Trans-stimulation experiment using diphenhydramine as a substrate

For the present trans-stimulation experiment, diphenhydramine was preloaded into cells by exposing them to the incubation medium (pH 6.0) containing 2 mM diphenhydramine for 10 min at 37 °C. The medium was removed, the cells were washed with 1.5 ml of incubation medium (pH 6.0), and the assay of the MDMA uptake was then measured for 1 min at 37 °C in 1.5 ml of incubation medium containing 100 μM MDMA.

2.5. Measurement of the MDMA efflux from preloaded cells

To evaluate the efflux rate of MDMA, the cells were preloaded with incubation medium (pH 7.4) containing 100 μM MDMA for 10 min at 37 °C. After removing the medium, the cells were washed with 1.5 ml of the incubation medium (pH 7.4), and then the assay of the MDMA remaining inside the cells was immediately initiated and continued for the designated time at 37 °C in 1.5 ml of the incubation medium (pH 6.0 or 7.4).

2.6. Effects of extracellular pH on the MDMA transport after the equilibrium distribution

The cells were first preloaded with incubation medium (pH 7.4) containing 100 μM MDMA for 15 min at 37 °C, and after equilibrium, 0.1 M NaOH (20 μl) was added into the incubation medium, bringing the pH value of the incubation medium to approximately 8.0. The cells were incubated for the designated time at 37 °C in the incubation medium to observe the further uptake of MDMA.

2.7. Permeation experiments by Caco-2 cell monolayers

The permeation experiment was performed in the incubation medium (pH 6.0 or 7.4) as the uptake experiment. After the culture medium was removed from both sides of cells and the cell surface was washed with 0.5 ml (apical side) and 1.0 ml (basolateral side) of the incubation medium prewarmed at 37 °C, the cells were preincubated in the same medium for 10 min at 37 °C. After the medium was removed, the apical and basolateral sides were incubated in the incubation medium with or without 50 μM MDMA for 90 min at 37 °C. Fifty microliters of the medium was taken from the apical or basolateral side at each designated time point (15, 30, 60, 90 min).

2.8. Measurement of MDMA taken up and permeated by Caco-2 cells

After the uptake experiments, the cells were frozen and thawed twice, and lysed cells were suspended in 400 μl of an extracting solution consisting of 25 mM ammonium acetate (pH 4.0) and acetonitrile in a volume ratio of 3:7 and 100 μM isoproterenol as an internal standard. After vigorous stirring, the extracting solution was transferred to a 1.5-ml microtube and shaken vigorously for 5 min, followed by centrifugation at 15,000×g for 5 min.

The supernatant was transferred to an autosampler vial for HPLC analysis. Twenty-five microliters of the supernatant was injected into an LC column equipped with a diode array detector (LC-10AD with SPD-M10A; Shimadzu, Kyoto, Japan). Chromatographic separation was achieved using a polymer-coated strong-cation exchange column (CAPCELL PAK SCX UG 80, 250 mM × 1.5 mM i.d.; Shiseido, Tokyo, Japan) at 40 °C. The mobile phase was 25 mM ammonium acetate (pH 4.0) and acetonitrile (3:7 in volume). The flow rate was maintained at 0.3 ml/min, and the monitoring wavelengths were 235 and 280 nm for MDMA and isoproterenol, respectively.

After the permeation experiments, the permeate obtained was diluted with 200 μl of a solution consisting of 25 mM ammonium acetate (pH 4.0) and acetonitrile in a volume ratio of 3:7 and 100 μM isoproterenol as an internal standard. The samples were analyzed as described above.

For all uptake measurements, values were corrected based on the protein contents. After the supernatant in the tube was removed, the precipitate was solubilized in 1 ml of 1 M NaOH to measure the protein contents. The protein contents of the cell monolayers were measured with a Bio-Rad protein assay kit (Bio-Rad Laboratories, Philadelphia, PA) using bovine serum albumin as a standard.

2.9. Kinetic analysis of MDMA uptake

The initial uptake rates of MDMA were estimated using linear regression analysis of the linear portion of the curve of uptake versus time. The data were fitted to a Michaelis–Menten type equation by an iterative nonlinear least-square method:

$$V = V_{max}[S]/(K_m + [S]) + K_d[S] \qquad (1)$$

where V represents the initial uptake rate of substrate; V_{max}, the maximum uptake velocity; $[S]$, the initial concentration of substrate; K_m, the Michaelis–Menten constant; and K_d, the coefficient of the passive diffusion. The initial uptake rates of MDMA were measured under various conditions, and the values were presented as the ratio of the MDMA uptake rate to the uptake rate of 100 μM MDMA in incubation medium (pH 6.0) without an inhibitor.

2.10. Measurement of intracellular pH

The intracellular pH of Caco-2 cells was measured using the fluorescent probe BCECF. Cells grown in 75-cm² culture flasks were trypsinized and suspended in the incubation medium (pH 7.4) at 1×10^7 cells/ml. Membrane-permeable BCECF-AM of 3 μM was added to the cell suspension, which was then incubated at 37 °C for 30 min. After the cells were washed twice with the incubation medium, the cells loaded with membrane-impermeable BCECF were suspended at 1×10^6 cells/ml in the incubation medium with various compounds for 10 min at 37 °C. The fluorescence intensity of BCECF was monitored using a spectrofluorophotometer (Shimadzu RF-5000) with excitation at 500 ± 5 nm and emission at 530 ± 5 nm. Intracellular pH was calibrated at different pH values between 6.2 and 8.2 using a calibration medium containing 130 mM KCl, 10 mM NaCl, 1 mM MgSO₄ and 10 mM MES, and containing 10 μg/ml nigericin.

3. Results

3.1. Carrier-mediated MDMA uptake by Caco-2 cells

The uptake of MDMA by Caco-2 cells was measured in the range of 0–30 min. Fig. 1 shows the time course for the uptake of 100 μM MDMA in the incubation medium (pH 6.0). Linearity is observed up to 3 min and the uptake reaches a plateau after 5 min. Because the uptake at time zero was the same as that at 4 °C, the uptake at time zero can be attributed to rapid adsorption to the cellular surface. Therefore, the initial uptake rate was calculated from the slope of the linear portion (0–3 min; see inset of Fig. 1).

Fig. 2 shows the relationship between the initial uptake rate and MDMA concentrations in the incubation medium (pH 6.0). The uptake was saturated at a high MDMA concentration. The inset in Fig. 2 shows an Eadie–Hofstee plot in which the line leans toward the lower right. The kinetic parameters were calculated by fitting the data to Eq. (1), and K_m and V_{max} were 1.11 ± 0.12 mM ($\pm$S.D.) and 13.79 ± 0.76 nmol/min/mg protein, respectively. It is noted that K_d was nearly zero, implying that the passive diffusion hardly contributed to the kinetics. The uptake rate of 100 μM MDMA at 4 °C (0.157 ± 0.037 nmol/min/mg protein) was much lower than that at 37 °C. As will be described later, compounds having an amine moiety similar to that of MDMA inhibited the uptake of
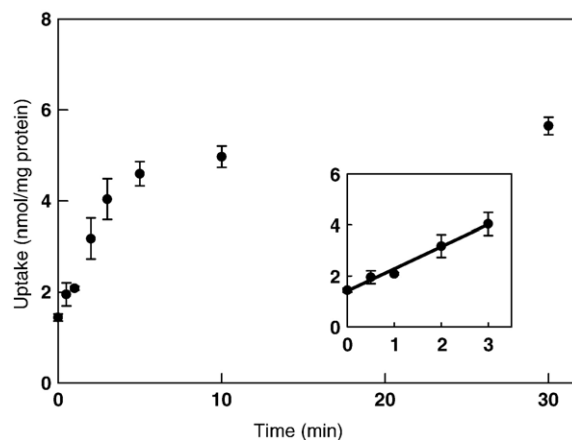

Fig. 1. Time course of the uptake of MDMA by Caco-2 cells. The uptake of 100 μM MDMA was measured at 37 °C in an incubation medium (pH 6.0) whose composition is described in the text. The inset enlarges the initial uptake, which is linear with time. Each point is the mean±S.E.M. of three experiments.
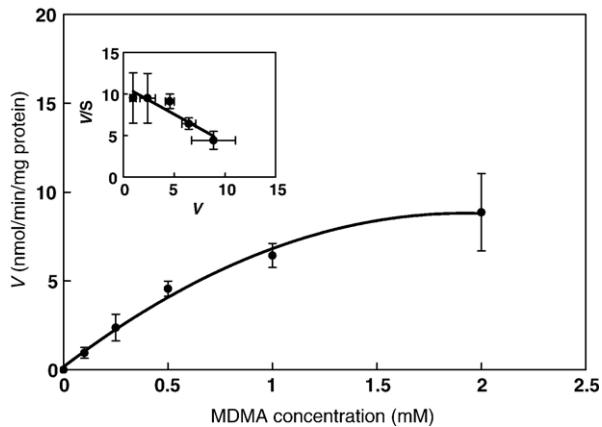
Fig. 2. Concentration dependence of the MDMA uptake rate by Caco-2 cells. The initial uptake rate was determined by linear regression analysis of the linear portion of the MDMA uptake versus time plot. The inset is an Eadie–Hofstee plot of the MDMA uptake. The experimental conditions were the same as those of Fig. 1. A fitting curve was drawn using the iterative nonlinear least-squares method. Each point is the mean±S.E.M. of three experiments.

MDMA. In addition, trans-stimulation was observed in the cells preloaded with the substrate diphenhydramine (see below). These findings reveal that MDMA uptake is mediated by a carrier protein.

3.2. MDMA uptake under various conditions

Uptake rates were measured under various conditions (see Fig. 3). First, we checked the dependency of the intracellular adenosine triphosphate (ATP) concentration. When the intracellular ATP level was reduced to approximately 20% of the control by the addition of 10 μM oligomycin together with 50 mM 2-deoxyglucose [25], the uptake rate showed almost no change. Various Na^+-dependent carriers, such as transporters of amino acids [16], sugars [17] and phosphates [18], have been reported. In the present study, we replaced Na^+ with Li^+ in the incubation medium, finding no change in MDMA uptake. Because the solubility of I^- in the lipid phase is approximately 20 times higher than that of Cl^-, the replacement of Cl^- with I^- in an extracellular medium creates a more negative membrane potential in an intracellular compartment [26]. However, this substitution had no observable effect, as shown in Fig. 3. The membrane potential-independent uptake was also confirmed by the observation that the addition of valinomycin (50 μM) to the medium had no effect on MDMA uptake (Fig. 3). MDMA uptake was partially inhibited by DEPC, which modified the histidine residues on the cells [27,28]. The results support the notion that MDMA transport is carrier-mediated. Based on these observations, we infer that this carrier-mediated MDMA
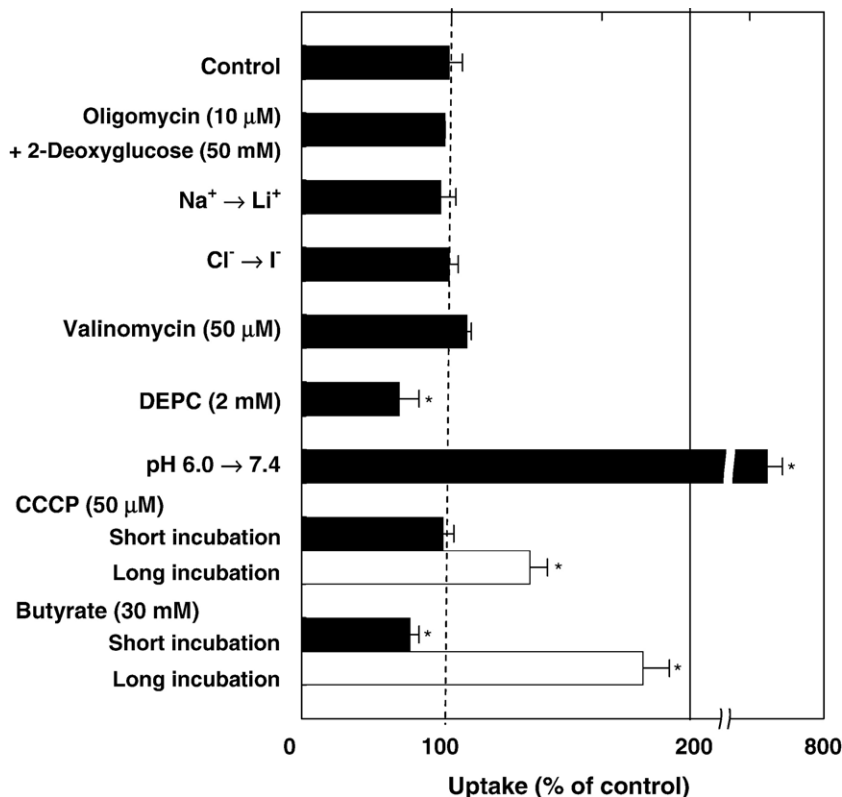

Fig. 3. Effects of various experimental conditions on MDMA uptake by Caco-2 cells. The uptake rate of 100 μM MDMA was measured in the incubation medium (pH 6.0 except for "pH 6.0→7.4") for 3 min at 37 °C under various conditions as described in the text. Arrows indicate that ion species in the incubation medium (pH 6.0) were replaced. "Short incubation" indicates that MDMA uptake was measured in the incubation medium (pH 6.0) containing 100 μM MDMA with 50 μM CCCP or 30 mM butyrate after the cells were preincubated in the incubation medium (pH 6.0) for 10 min at 37 °C. "Long incubation" indicates that MDMA uptake was measured in the incubation medium (pH 6.0) containing 100 μM MDMA without CCCP or butyrate after the cells were preincubated with 1.5 ml of the incubation medium (pH 6.0) containing 50 μM CCCP or 30 mM butyrate for 30 min at 37 °C. Statistical analysis was done by Student's t-test. *$P < 0.05$ versus the control. Each value is the mean±S.E.M. of three experiments.

transport is neither supported by ATP hydrolysis, nor Na^+ dependent, but rather is an electroneutral process.

In contrast, we observed significant pH dependence, as shown in Fig. 3. When the pH of the incubation medium was increased from 6.0 to 7.4, MDMA uptake increased significantly. To examine the coupling of the proton electrochemical potential, the protonophore, CCCP, was added to the incubation medium (pH 6.0) containing MDMA. However, we observed no effect (Fig. 3), indicating that this transport is not driven by the difference in the proton electrochemical difference, that is, the proton motive force. The uptake of MDMA was enhanced only when CCCP was preincubated for a long time (30 min). Therefore, we must distinguish between two CCCP treatments based on whether they involve a 'short' or 'long' incubation. Short incubation of CCCP did not affect the uptake rate.

3.3. Effects of intra- and extracellular pH on uptake and efflux of MDMA

Having observed the effect of extracellular pH on uptake (Fig. 3), we next examined the effect of intracellular pH. We used treatment with NH_4Cl to change the intracellular pH levels. Exposure of the cells to NH_4Cl (acute NH_4Cl) has been found to cause a rapid increase in pH [29]. As shown in Fig. 4, this treatment (causing intracellular alkalinization) decreases the uptake rate, while the pre-NH_4Cl treatment (causing intracellular acidification) increases uptake. Details of both treatments are given above in the Materials and methods section.

Another method of changing intracellular pH is to use a weak acid, butyrate (30 mM); a neutral form of butyrate may enter the intracellular space, where the acid may dissociate and thus decrease pH. However, when 30 mM of butyrate was added in the present experiments, only a slight inhibition was observed on the uptake rate (see short incubation of butyrate in Fig. 3).
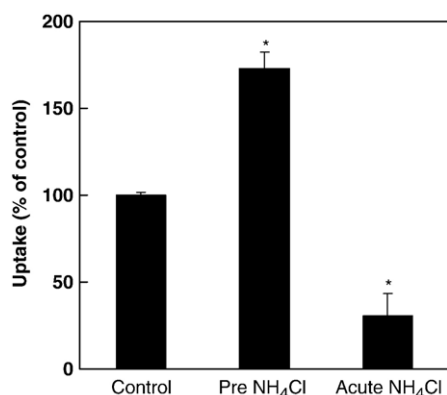

Fig. 4. Effect of NH_4Cl treatment on MDMA uptake by Caco-2 cells. The cells were preincubated for 10 min at 37 °C with the incubation medium (pH 7.4) in the absence (control, acute NH_4Cl) or presence (pre-NH_4Cl) of 30 mM NH_4Cl. After removing the medium, the cells were incubated for 3 min at 37 °C with 1.5 ml of incubation medium (pH 7.4) containing 100 μM MDMA in the absence (control, pre-NH_4Cl) or presence (acute NH_4Cl) of 30 mM NH_4Cl. The uptake of MDMA was measured in each incubation medium. See the text for a discussion of the intracellular pH changes brought about by this treatment. Statistical analysis was performed using the Student's t-test. *$P < 0.05$ versus the control. Each value is the mean±S.E.M. of three experiments.
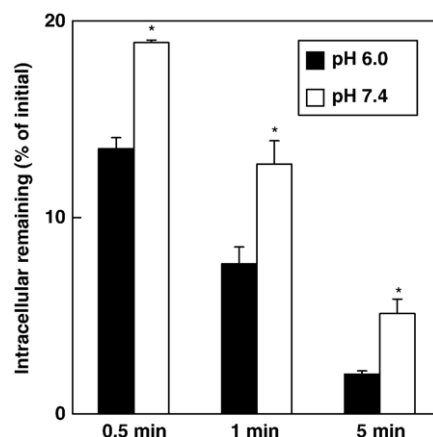

Fig. 5. MDMA efflux from preloaded Caco-2 cells. The cells were preloaded with incubation medium (pH 7.4) containing 100 μM MDMA for 10 min at 37 °C. After the medium was removed, the cells were washed with 2 ml of the incubation medium (pH 7.4) at 37 °C, and then immediately treated for the designated time (0.5, 1 or 5 min) at 37 °C with 1.5 ml of the incubation medium (pH 6.0 or 7.4). The amounts of MDMA remaining in the cells were measured. Statistical analysis was carried out using the Student's t-test. *$P < 0.05$ versus the control (pH 6.0). Each value is the mean±S.E.M. of three experiments.

However, when the cells were incubated in the presence of 30 mM butyrate for 30 min, an increase in the uptake rate was observed (see long incubation of butyrate in Fig. 3), and intracellular pH decreased from 6.94 ± 0.03 to 6.55 ± 0.03, as estimated by BCECF. The reason that such a long incubation is required in order for an effect to be discernible may be that butyric acid is transported very slowly. Another possibility is that butyrate may be metabolized to other acidic substances.

We observed a similar effect on CCCP. As described above, a short incubation period of CCCP did not produce any effect (see short incubation of CCCP in Fig. 3). However, long incubation (for approximately 30 min) resulted in an appreciable increase in the uptake rate (see long incubation of CCCP in Fig. 3). We considered it very strange that the presence of CCCP, which is an uncoupler, enhances the uptake rate. Therefore, we measured intracellular pH with BCECF [30], which decreased as expected to 6.64 ± 0.02. The addition of CCCP for 30 min would modulate the proton-coupled transporters of the cell membrane to change the intracellular pH, while a shorter application of CCCP would not be expected to bring about any significant change in pH.

MDMA efflux was measured from preloaded cells, and the results are shown in Fig. 5. Efflux rates were found to increase as extracellular pH decreased. Thus, the outwardly directed proton concentration gradient accelerates the uptake of MDMA while a proton gradient in the reverse direction accelerates the efflux, indicating an antiport system in which both protons and MDMA participate. In addition, the effects of extracellular pH on the equilibrium of MDMA distribution by Caco-2 cells were examined (Fig. 6). After MDMA in Caco-2 cells reached equilibrium by incubating the cells in MDMA-containing medium (pH 7.4) at 37 °C for 15 min, NaOH was added to the incubation medium. The increase of the extracellular pH led to the uptake of MDMA. This observation also implies that this antiporter can concentrate MDMA by an outwardly directed proton gradient.
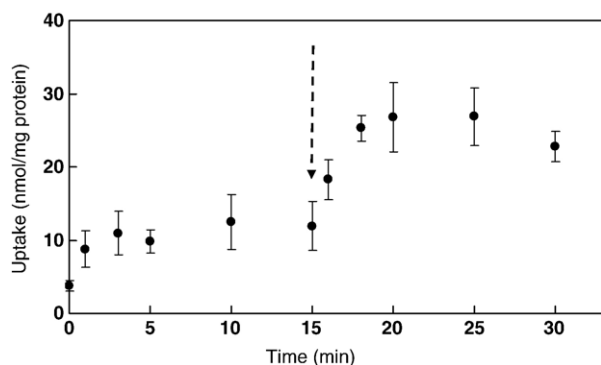
Fig. 6. Effects of extracellular pH on the equilibrium of MDMA distribution by Caco-2 cells. The uptake of 100 μM MDMA was measured in the incubation medium (pH 7.4) at 37 °C for 15 min, allowing the MDMA distribution to attain equilibrium, and the extracellular pH level was then changed to approximately 8.0 by the addition of 0.1 M NaOH (20 μl) to the incubation medium. The arrow represents the addition of aqueous NaOH. Each point is the mean±S.E.M. of three experiments.

3.4. Permeation of MDMA through Caco-2 cells

The permeations of MDMA from the apical to the basolateral side (from A to B) or from the basolateral to the apical side (from B to A) through Caco-2 cells were measured in the range of 15–90 min (Fig. 7). The linearity of permeation in both directions was observed up to 90 min. The permeation rate was determined by linear regression analysis of the permeation plot from 15 to 90 min. When an H^+ concentration gradient from A (pH 6.0) to B (pH 7.4) was created, the rate of permeation from B to A was approximately 10 times higher than that of permeation from A to B, and even without an H^+ concentration gradient (pH 7.4 on both sides), the rate of permeation from B to A was approximately 1.4 times higher than that of permeation from A to B. These facts imply that the efflux of MDMA is superior to the uptake under physiological conditions (see later discussion and Fig. 10). Nevertheless, we observed a transport from the apical to the basolateral side.

3.5. Specificity of MDMA uptake

We examined the effects of various compounds (1 mM) on 100 μM of MDMA uptake (Table 1). When ATSs such as MDA and MDEA, whose chemical structures are similar to that of MDMA, were added to the incubation medium containing MDMA, uptake was inhibited, and MDEA greatly inhibited MDMA uptake in comparison with the other compounds. Various cationic drugs and compounds in ATS tablets were also examined. Diphenhydramine was found to strongly inhibit MDMA uptake in all tested compounds other than ATSs, while caffeine, which is frequently included in ATS tablets, did not change the MDMA uptake.

To evaluate the inhibition of MDMA uptake by diphenhydramine, a Dixon plot was generated (Fig. 8). The inhibition of MDMA uptake by diphenhydramine was competitive, and K_i, which was estimated using the intersection of the lines obtained from two concentrations of MDMA, was found to be approximately 2 mM, a value which was similar to the K_m value of MDMA uptake. Moreover, a trans-stimulation experiment was performed using cells preloaded with diphenhydramine in order to determine whether MDMA is taken up though the transporter. The uptake of MDMA at 1 min was significantly enhanced ($136.7\pm9.0\%$ ($n=3$)) compared to the control by preloading with
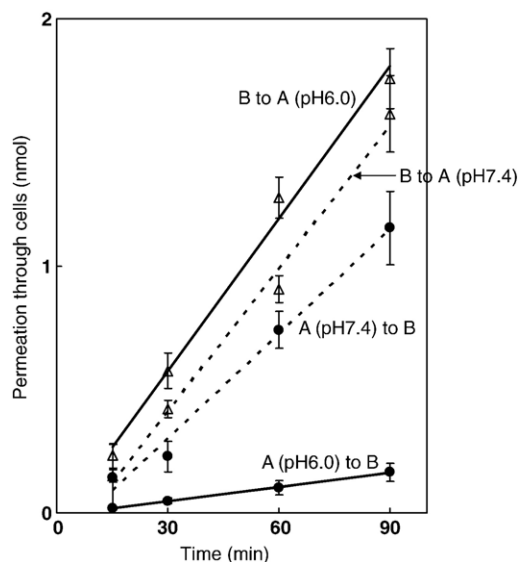

Fig. 7. Time courses of the permeations of MDMA from the apical to the basolateral side and from the basolateral to the apical side through Caco-2 cells. After the incubation medium (pH 6.0 or 7.4) containing 50 μM MDMA was added to the apical or basolateral side, the permeation was measured for 90 min. "A (pH 6.0) to B" indicates that the incubation medium (pH 6.0) containing MDMA was added to the apical side, and then the permeation of MDMA to the basolateral side (pH 7.4) was measured. The permeation rate was determined by linear regression analysis of the permeation plot from 15 to 90 min. Each point is the mean±S.E.M. of three experiments.

Table 1
Inhibitory effects of various compounds on MDMA uptake

Compounds	Uptake (percent of control)
MDA	59.4 ± 16.5*
MDEA	39.6 ± 2.1*
MA	73.7 ± 9.0*
EP	87.3 ± 2.1*
DMA	59.0 ± 2.7*
Ketamine	79.0 ± 10.1*
Diphenhydramine	65.1 ± 0.4*
Clonidine	76.4 ± 6.0*
Caffeine	98.8 ± 2.2
TEA	100.4 ± 7.7
MPP^+	90.0 ± 7.7
Guanidine	93.5 ± 3.1
Verapamil	91.7 ± 6.4
β-Phenetylamine	59.8 ± 2.7*
4-Phenyl-1-butanamine	32.1 ± 4.4*
Tyramine	75.3 ± 7.3*
Phenylalanine	103.8 ± 11.4
Tyrosine	104.0 ± 9.2

The uptake rates of 100 μM MDMA were measured in the absence or presence of various compounds (1 mM). Experimental conditions were as described in the text. Statistical analysis was done by Student's t-test.
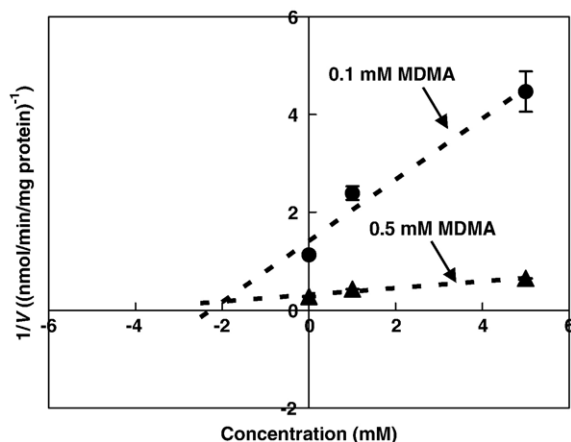 * $P<0.05$ vs. the control (pH 6.0). Each value is the mean±S.E.M. of three experiments.

Fig. 8. Concentration-dependent inhibition of MDMA uptake by diphenhydramine. The uptake rates of MDMA at two concentrations (0.1 and 0.5 mM) were measured in the incubation medium (pH 6.0) at 37 °C in the absence or presence of diphenhydramine (1 or 5 mM). A Dixon plot of MDMA uptake against diphenhydramine concentrations was generated. The lines at each concentration of MDMA were drawn by linear regression analysis. Each point is the mean± S.E.M. of three experiments.

10 mM diphenhydramine. This suggests that MDMA and diphenhydramine are transported by a common carrier.

Mizuuchi et al. demonstrated that diphenhydramine is transported by the pH-dependent tertiary amine transport system in Caco-2 cells [29] and in rabbit intestinal brush border membrane vesicles [31]. The transport system is able to recognize N-dimethyl or N-diethyl moieties in the structures. MDMA is, however, a secondary amine that possesses an N-methyl moiety in its structure.

Organic cation transporters (OCT) 1, 2 and 3 mediate the facilitated transport of a variety of structurally diverse organic cations and are broadly expressed in the liver, kidney and intestine [32]. Tetraethylammonium (TEA) and 1-methyl-4-phenylpyridinium (MPP$^+$) [33], typical substrates of OCTs, did not inhibit MDMA uptake in the present experiments. On the other hand, tyramine, which is a substrate for rat OCT-1 and human OCT-3, was found to inhibit the uptake. Although a guanidine/H$^+$ antiporter in intestinal brush border membrane vesicles has been reported [34], guanidine did not inhibit MDMA uptake in the present study. Verapamil, a P-glycoprotein substrate [35], had no effect on MDMA uptake. In addition, because MDMA uptake is ATP-independent, P-glycoprotein is believed to have no relation with MDMA uptake. Recently, a proton-coupled efflux transporter (MATE) was reported [36–38]. The substrates of MATE are different from those of this transport system. Although the spectrum of substrate recognition in the present case seems to be different from that of many transport systems reported previously [36–41], the specificity and mechanism of MDMA were similar to those of the clonidine uptake reported recently [42].

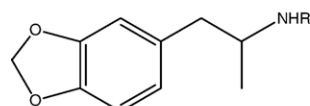### 3.6. Relationship between structure and the recognition of the MDMA transport system

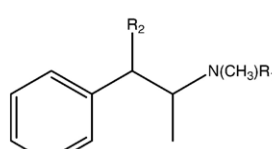Substrate recognition was examined using various compounds having structures similar to that of MDMA. All compounds that inhibited MDMA uptake possessed aliphatic amino moieties. Fig. 9 shows the structures of MDMA-related compounds tested in the present study. Although the structures of diphenhydramine, ketamine and clonidine differ greatly from that of MDMA, these compounds seem to be recognized by the MDMA transport system because of the presence of an aliphatic amino moiety. The inhibitory effects tended to become larger in the order of primary, secondary and tertiary amine moiety judging from the comparison of MDA with MDEA, and of MA with DMA. Quaternary ammonium compounds such as TEA and MPP$^+$ did not, however, inhibit MDMA uptake at all.

As the carbon chain of the aliphatic amino moiety was longer, the inhibition against MDMA uptake was greater (Table 1, β-phenethylamine and 4-phenyl-1-butanamine). and tyrosine, neutral aromatic amino acids, did not inhibit MDMA uptake. EP, MA having a 2-hydroxy moiety, and tyramine, β-phenethylamine having a p-hydroxyl moiety, showed a weaker inhibition against MDMA uptake than MA and β-phenethylamine, respectively. Thus, carboxyl and hydroxyl moieties were considered to interfere with the recognition of the transport system.

4. Discussion

The present paper reveals, for the first time, that MDMA can be transported by an electroneutral proton-coupled transport system. Since the pK_a value of MDMA is 10.1 [43], almost all MDMA molecules are present in a positively charged form. Because of the electroneutral transport, the transport system should be an antiporter with H$^+$ in the ratio of 1:1. Our present results show that alkalinization of extracellular pH or acidification of intracellular pH increases the uptake rate, that is, an increase in the gradient of the outward proton concentration increases the uptake rate. This experimental finding may suggest that MDMA uptake is mediated by an antiporter driven by the outward movement of H$^+$.
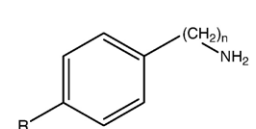
Fig. 9. The chemical structures of MDMA and its related compounds tested in the present study.

Under the physiological conditions as well as the present experimental condition of a medium pH of 6.0, however, this process should not occur because the proton concentration gradient is in the reverse direction due to the acidic pH microclimate [40,44]. What, then, is the mechanism of MDMA uptake? We assume the transport cycle shown in Fig. 10. In this figure, X^-, XH and XS indicate the empty transporter, the protonated transporter and the substrate-associated transporter, respectively. Since the transport is electroneutral, and since the pH in both the extracellular and intracellular spaces regulates the transport rate, we assume here that the empty transporter bears a negatively dissociated amino acid residue denoted by X^-, with which H^+ or S^+ binds. Note that the pK_a value of MDMA is 10.1, and that MDMA is then protonated and positively charged as denoted by S^+. As the intracellular pH decreases, the $X^- \leftrightarrow$ XH reaction at the intracellular membrane surface shifts to a decrease in X^-, giving rise to an acceleration of the release of S^+. A similar but reverse pH dependence occurs on the extracellular side.

Furthermore, we assume that this transport system is reversible (Fig. 5), meaning that the transport cycle shown in Fig. 10 can rotate either clockwise or counter-clockwise depending on the magnitude of the proton gradient and the substrate concentration gradient. If $\{[H^+]_{out} - [H^+]_{in}\} \gg \{[S^+]_{out} - [S^+]_{in}\}$, this transport system functions as a proton-coupled efflux pump (antiporter with proton; clockwise rotation in Fig. 10). Note that under the usual physiological conditions, the relation $[H^+]_{out} > [H^+]_{in}$ usually holds. Nevertheless, if the relation $\{[S^+]_{out} - [S^+]_{in}\} \gg \{[H^+]_{out} - [H^+]_{in}\}$ holds, the uptake of substrate S^+ that follows its concentration gradient may occur due to the reverse rotation of the transport cycle of the antiporter, i.e., by a counter-clockwise rotation of the transport cycle shown in Fig. 10. Such a bidirectional transport has been demonstrated in other transporters [45–47]. This condition holds at present, because $\{[H^+]_{out} - [H^+]_{in}\}$ is approximately on the order of μM while $\{[S^+]_{out} - [S^+]_{in}\}$ is 0.1 to 2 mM. When we confine ourselves to the movement of the substrate, it may be said that the uptake of substrate is mediated by a 'facilitated transporter'.

If the transport system shown in Fig. 10 is indeed present it may be possible to allow the transport system to function as an antiporter with H^+, as discussed above. This was done in the present study and the results are shown in Fig. 6. First, MDMA was loaded into cells under the condition of an equivalent pH inside and outside cells. After the MDMA distribution reached equilibrium, the extracellular pH was increased to create a proton gradient from the inside to the outside of the cells. As shown in Fig. 10, this pH change induces the further uptake of MDMA, which is consistent with the scheme shown in the figure. After 25 min, the intracellular MDMA decreased, possibly due to the efflux of MDMA in accordance with its concentration difference. This suggests the reversibility of the transport system.

As mentioned above, the clockwise rotation of the transport cycle indicates a proton-coupled efflux pump, which is more likely under the physiological conditions than the 'facilitated transporter'. The results in Fig. 7 support the notion that this transport system functions as a proton-coupled efflux pump.
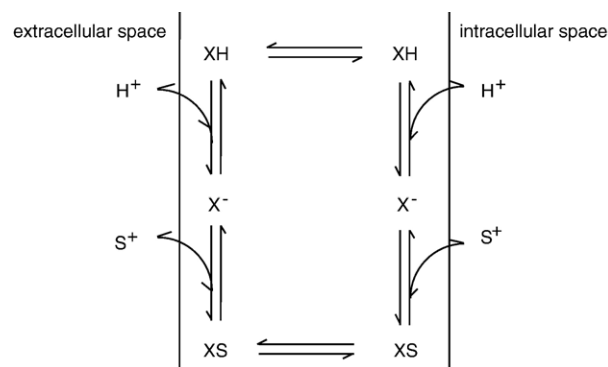

Fig. 10. The presumptive transport mechanism of MDMA uptake. X^-, XH and XS indicate the empty transporter, the protonated transporter and the substrate-associated transporter, respectively. For details, see Discussion.

Moreover, Fig. 7 implies that the pH changes of the acidic microclimate on the apical membrane affect the transport system. We must take this transport system into consideration when we examine the bioavailability of drugs having an amine moiety, because this transport system might serve as a proton-coupled efflux transport system under certain conditions, and function as a proton-moving facilitated transporter under other conditions. In addition, based on the observed substrates, the present transport system might be a novel one. Here, we did not pay attention to lysosomal trapping of alkaline compounds because we focused on the initial uptake over the short term. This accumulation, however, should be considered when the distribution of MDMA is investigated. In addition, further investigation will be needed into such issues as molecular cloning and biochemical characterization.

References

[1] National Police Agency of Japan, White Paper on Police, National Police Agency of Japan, Tokyo, 2005, pp. 191–192.

[2] Y. Makino, S. Tanaka, S. Kurobane, M. Nakauchi, T. Terasaki, S. Ohta, Profiling of illegal amphetamine-type stimulant tablets in Japan, J. Health Sci. 49 (2003) 129–137.

[3] H. Kalant, The pharmacology and toxicology of "ecstasy" (MDMA) and related drugs, CMAJ 165 (2001) 917–928.

[4] T.A. Dal Cason, An evaluation of the potential for clandestine manufacture of 3,4-methylenedioxyamphetamine (MDA) analogs and homologs, J. Forensic Sci. 35 (1990) 675–697.

[5] V. Fineschi, A. Masti, Fatal poisoning by MDMA (ecstasy) and MDEA: a case report, Int. J. Leg. Med. 108 (1996) 272–275.

[6] K. Ahmad, Increased use of amphetamine-type stimulants threatens east Asian countries, Lancet 359 (2002) 1927.

[7] K. Wolff, A.W. Hay, K. Sherlock, M. Conner, Contents of "ecstasy", Lancet 346 (1995) 1100–1101.

[8] K.L. Jansen, R. Darracot-Cankovic, The nonmedical use of ketamine, part two: a review of problem use and dependence, J. Psychoact. Drugs 33 (2001) 151–158.

[9] K.M. Bertelsen, D.J. Greenblatt, L.L. von Moltke, Apparent active transport of MDMA is not mediated by P-glycoprotein: a comparison with MDCK and Caco-2 monolayers, Biopharm. Drug Dispos. 27 (2006) 219–227.

[10] S. Seidel, E.A. Singer, H. Just, H. Farhan, P. Scholze, O. Kudlacek, M. Holy, K. Koppatz, P. Krivanek, M. Freissmuth, H.H. Sitte, Amphetamines take two to tango: an oligomer-based counter-transport model of neurotransmitter transport explores the amphetamine action, Mol. Pharmacol. 67 (2005) 140–151.

[11] C. Pifl, G. Nagy, S. Berenyi, A. Kattinger, H. Reither, S. Antus, Pharmacological characterization of ecstasy synthesis byproducts with recombinant human monoamine transporters, J. Pharmacol. Exp. Ther. 314 (2005) 346–354.

[12] N.K. Kiyanvash, J. Weiss, W.E. Haefeli, G. Mikus, P-glycoprotein modulation by the designer drugs methylendioxymethamphetamine, methylenedioxyethylamphetamine and paramethoxyamphetamine, Addict. Biol. 8 (2003) 413–418.

[13] H. Mann, B. Ladenheim, H. Hirata, T.H. Moran, J.L. Cadet, Differential toxic effects of methamphetamine (METH) and methylenedioxymethamphetamine (MDMA) in multidrug-resistant (mdr1a) knockout mice, Brain Res. 769 (1997) 340–346.

[14] I.J. Hidalgo, T.J. Raub, R.T. Borchardt, Characterization of the human colon carcinoma cell line (Caco-2) as a model system for intestinal epithelial permeability, Gastroenterology 96 (1989) 736–749.

[15] A.R. Hilgers, R.A. Conradi, P.S. Burton, Caco-2 cell monolayers as a model for drug transport across the intestinal mucosa, Pharm. Res. 7 (1990) 902–910.

[16] I.J. Hidalgo, R.T. Borchardt, Transport of a large neutral amino acid (phenylalanine) in a human intestinal epithelial cell line: Caco-2, Biochim. Biophys. Acta 1028 (1990) 25–30.

[17] P. Bissonnette, H. Gagne, M.J. Coady, K. Benabdallah, J.Y. Lapointe, A. Berteloot, Kinetic separation and characterization of three sugar transport modes in Caco-2 cells, Am. J. Physiol. 270 (1996) G833–G843.

[18] I. Mohrmann, M. Mohrmann, J. Biber, H. Murer, Sodium-dependent transport of Pi by an established intestinal epithelial cell line (CaCo-2), Am. J. Physiol. 250 (1986) G323–G330.

[19] I.J. Hidalgo, R.T. Borchardt, Transport of bile acids in a human intestinal epithelial cell line, Caco-2, Biochim. Biophys. Acta 1035 (1990) 97–103.

[20] M. Brandsch, Y. Miyamoto, V. Ganapathy, F.H. Leibach, Expression and protein kinase C-dependent regulation of peptide/H^+ co-transport system in the Caco-2 human colon carcinoma cell line, Biochem. J. 299 (Pt 1) (1994) 253–260.

[21] H. Daniel, C. Fett, A. Kratz, Demonstration and modification of intervillous pH profiles in rat small intestine in vitro, Am. J. Physiol. 257 (1989) G489–G495.

[22] T. Inoue, S. Suzuki, Studies on metabolism of methamphetamine analogs 6. Analysis of dimethylamphetamine and its metabolites, Rep. Natl. Res. Inst. Police Sci. 39 (1986) 228–234.

[23] K. Tanaka, T. Inoue, H. Ohki, Analysis of 3,4-methylenedioxymethamphetamine and its metabolites, Rep. Natl. Res. Inst. Police Sci. 41 (1988) 22–27.

[24] T. Kanamori, K. Tanaka, Y. Togawa, T. Inoue, Analysis of 3,4-methylenedioxyamphetamine and its N-alkyl analogues, Rep. Natl. Res. Inst. Police Sci. 51 (1998) 32–41.

[25] K. Kuwayama, S. Miyauchi, R. Tateoka, H. Abe, N. Kamo, Fluorescein uptake by a monocarboxylic acid transporter in human intestinal Caco-2 cells, Biochem. Pharmacol. 63 (2002) 81–88.

[26] S.H. Wright, T.M. Wunz, Transport of tetraethylammonium by rabbit renal brush-border and basolateral membrane vesicles, Am. J. Physiol. 253 (1987) F1040–F1050.

[27] M. Brandsch, C. Brandsch, M.E. Ganapathy, C.S. Chew, V. Ganapathy, F.H. Leibach, Influence of proton and essential histidyl residues on the transport kinetics of the H^+/peptide cotransport systems in intestine (PEPT 1) and kidney (PEPT 2), Biochim. Biophys. Acta 1324 (1997) 251–262.

[28] Y. Fujisawa, R. Tateoka, T. Nara, N. Kamo, T. Taira, S. Miyauchi, The extracellular pH dependency of transport activity by human oligopeptide transporter 1 (hPEPT1) expressed stably in Chinese hamster ovary (CHO) cells: a reason for the bell-shaped activity versus pH, Biol. Pharm. Bull. 29 (2006) 997–1005.

[29] H. Mizuuchi, T. Katsura, K. Ashida, Y. Hashimoto, K. Inui, Diphenhydramine transport by pH-dependent tertiary amine transport system in Caco-2 cells, Am. J. Physiol.: Gasterointest. Liver Physiol. 278 (2000) G563–G569.

[30] J.A. Thomas, Intracellularly trapped pH indicators, Soc. Gen. Physiol. Ser. 40 (1986) 311–325.

[31] T. Katsura, H. Mizuuchi, Y. Hashimoto, K. Inui, Transport of procainamide via $H(+)$/tertiary amine antiport system in rabbit intestinal brush-border membrane, Am. J. Physiol. Gasterointest. Liver Physiol. 279 (2000) G799–G805.

[32] J.W. Jonker, A.H. Schinkel, Pharmacological and physiological functions of the polyspecific organic cation transporters: OCT1, 2, and 3 (SLC22A1–3), J. Pharmacol. Exp. Ther. 308 (2004) 2–9.

[33] M.K. Kim, C.K. Shim, The transport of organic cations in the small intestine: current knowledge and emerging concepts, Arch. Pharm. Res. 29 (2006) 605–616.

[34] Y. Miyamoto, V. Ganapathy, F.H. Leibach, Transport of guanidine in rabbit intestinal brush-border membrane vesicles, Am. J. Physiol. 255 (1988) G85–G92.

[35] T.J. Raub, P-glycoprotein recognition of substrates and circumvention through rational drug design, Mol. Pharmacol. 3 (2006) 3–25.

[36] H. Omote, M. Hiasa, T. Matsumoto, M. Otsuka, Y. Moriyama, The MATE proteins as fundamental transporters of metabolic and xenobiotic organic cations, Trends Pharmacol. Sci. 27 (2006) 587–593.

[37] T. Terada, S. Masuda, J. Asaka, M. Tsuda, T. Katsura, K. Inui, Molecular cloning, functional characterization and tissue distribution of rat H^+/organic cation antiporter MATE1, Pharm. Res. 23 (2006) 1696–1701.

[38] K.Y. Ohta, K. Inoue, Y. Hayashi, H. Yuasa, Molecular identification and functional characterization of rat multidrug and toxin extrusion type transporter 1 as an organic cation/H^+ antiporter in the kidney, Drug Metab. Dispos. 34 (2006) 1868–1874.

[39] E.M. Wright, D.D. Loo, Coupling between Na^+, sugar, and water transport across the intestine, Ann. N.Y. Acad. Sci. 915 (2000) 54–66.

[40] V. Ganapathy, M.E. Ganapathy, F.H. Leibach, Intestinal transport of peptides and amino acids, Academic Press, New York, 2001, pp. 379–419.

[41] L.M. Chan, S. Lowes, B.H. Hirst, The ABCs of drug transport in intestine and liver: efflux proteins limiting drug absorption and bioavailability, Eur. J. Pharm. Sci. 21 (2004) 25–51.

[42] W. Fischer, L. Metzner, K. Hoffmann, R.H. Neubert, M. Brandsch, Substrate specificity and mechanism of the intestinal clonidine uptake by Caco-2 cells, Pharm. Res. 23 (2006) 131–137.

[43] R. Torre, M. Farre, M. Navarro, R. Pacifici, P. Zuccaro, S. Pichini, Clinical pharmacokinetics of amfetamine and related substances: monitoring in conventional and non-conventional matrices, Clin. Pharmacokinet. 43 (2004) 157–185.

[44] I.J. Hidalgo, K.M. Hillgren, G.M. Grass, R.T. Borchardt, Characterization of the unstirred water layer in Caco-2 cell monolayers using a novel diffusion apparatus, Pharm. Res. 8 (1991) 222–227.

[45] G. Kottra, A. Stamfort, H. Daniel, PEPT1 as a paradigm for membrane carriers that mediate electrogenic bidirectional transport of anionic, cationic, and neutral substrates, J. Biol. Chem. 277 (2002) 32683–32691.

[46] M. Foltz, M. Mertl, V. Dietz, M. Boll, G. Kottra, H. Daniel, Kinetics of bidirectional H^+ and substrate transport by the proton-dependent amino acid symporter PAT1, Biochem. J. 386 (2005) 607–616.

[47] Y. Fujisawa, T. Kitagawa, M. Miyake, T. Nara, N. Kamo, S. Miyauchi, Measurement of electric current evoked by substrate transport via bidirectional $H(+)$/oligopeptide transporter over-expressed in HeLa cells: electrogenic efflux and existence of a newly observed channel-like state, Arch. Biochem. Biophys. 445 (2006) 166–173.